Arabian Journal of Chemistry (2020) 13, 2101–2109

King Saud University

Arabian Journal of Chemistry

www.ksu.edu.sa
www.sciencedirect.com

ORIGINAL ARTICLE

Flurbiprofen conjugates based on hydroxyethylcellulose: Synthesis, characterization, pharmaceutical and pharmacological applications

Khawar Abbas [a], Muhammad Ajaz Hussain [a,*], Syed Nasir Abbas Bukhari [b], Muhammad Amin [a], Muhammad Nawaz Tahir [c,*], Sheshanath V. Bhosale [d,1]

[a] *Ibn-e-Sina Block, Department of Chemistry, University of Sargodha, Sargodha 40100, Pakistan*
[b] *Department of Pharmaceutical Chemistry, College of Pharmacy, Jouf University, Aljouf, Sakaka 2014, Saudi Arabia*
[c] *Chemistry Department, King Fahd University of Petroleum and Minerals, Dhahran 31261, Saudi Arabia*
[d] *School of Science, RMIT University, GPO BOX 2476, Melbourne, VIC 3001, Australia*

Received 25 December 2017; accepted 14 March 2018
Available online 21 March 2018

KEYWORDS

Hydroxyethylcellulose;
Flurbiprofen;
Prodrug;
Immunomodulatory assay;
Anti-inflammatory activity

Abstract Present study deals with fabrication of macromolecular prodrugs (MPDs) of flurbiprofen (FLB) with hydroxyethylcellulose (HEC). FLB was activated using *p*-toluenesulfonyl chloride and reacted with pre-dissolved HEC to yield HEC-FLB conjugates **1**–**3**. Resultant prodrugs showed moderate to high degree of substitution (DS: 0.40–1.74) and assembled into nanoparticles of 220–550 nm at water/DMSO interface. Pharmacokinetic studies of HEC-FLB conjugate revealed a t_{max} of 4.0 h indicating delayed release of FLB while $t_{1/2}$ of 10.63 h indicated sustained release characteristics of the conjugate in rabbit model. Pharmacological studies revealed that HEC-FLB conjugates had immunomodulatory potential as results showed 34 and 36% inhibition of Interleukin-6 and tumor necrosis factor-α, respectively. A 79% inhibition of paw edema indicated anti-inflammatory properties of the conjugates. Cell viability studies indicated safety of the conjugates to L929 cell lines up to 24 h in the range of 2–10 mM. Moreover, thermal analysis indicated greater stability of MPDs than FLB.

1. Introduction

Flurbiprofen (FLB) is a 2-phenylpropionic acid derivative and belongs to a widely prescribed class of drugs, i.e., non-steroidal anti-inflammatory drugs (NSAIDs). It is commonly used as an analgesic, antipyretic and anti-inflammatory agent. But its prolonged use is associated with a number of side effects like gastrointestinal irritation, abdominal pain, dyspepsia, nausea,

* Corresponding authors.
E-mail addresses: majaz172@yahoo.com (M.A. Hussain), muhammad.tahir@kfupm.edu.sa (M.N. Tahir).
[1] Present address: Department of Chemistry, Goa University, Taleigao Plateau, Goa 403 206, India.
Peer review under responsibility of King Saud University.

Production and hosting by Elsevier

https://doi.org/10.1016/j.arabjc.2018.03.011
1878-5352

vomiting and in severe cases ulceration and hemorrhage (Gabriel et al., 1991; Halen et al., 2009).

In order to reduce the side effect of NSAIDs, it is common practice to mask their carboxyl groups by converting into their bioreversible derivatives. This approach not only allows reduction of gastric irritancy caused by acid containing drugs (Halen et al., 2006) but also provides a pathway to achieve intestine targeted drug delivery (Mørk and Bundgaard, 1992). Literature has shown that FLB has been converted to amide, amino acid and glycolamide ester derivatives (Mørk and Bundgaard, 1992) to reduce its side effects. However, no effort has been made to fabricate prodrugs of FLB on to polysaccharide materials.

Polysaccharides are amongst the materials of interest in drug design and delivery systems due to their structural diversity and flexible nature towards chemical modification. Fabrication of prodrugs using polysaccharide materials has several advantages such as increased solubility of hydrophobic drugs, improved bio-distribution, prolonged therapeutic levels and increased selectivity for the target receptors (Harboe et al., 1988; Larsen 1990; Abbas et al., 2016; Xu et al., 2015; Li et al., 2017; Li et al., 2016). Amongst polysaccharides, HEC is a prime candidate for fabrication of novel MPDs due to its hydrophilic and biocompatible nature. Recently, salicylic acid, aspirin and ibuprofen prodrugs based on HEC (Abbas et al., 2017b; Abbas et al., 2017a) have been reported where useful results were obtained. Some of the other studies highlighted the use of HEC as a potential carrier for fluoroquinolone antibiotics (Amin et al., 2015; Abbas et al., 2016).

Keeping in mind the potential properties of HEC as a novel drug carrier, we were interested to fabricate prodrugs of FLB on to HEC. The resultant conjugates were expected to afford sustained release of FLB owing to enzymatic hydrolysis *in vivo*, so pharmacokinetic studies of the HEC-FLB conjugates were undertaken in albino rabbits. We were also aimed at evaluation of anti-inflammatory, immunomodulatory and cytotoxic profiles of FLB conjugates to assess their therapeutic efficacy. Thermal analysis of the synthesized conjugates was also undertaken to assess their thermal stability.

2. Materials and methods

2.1. Materials

HEC (Natrosol, hydroxyethylcellulose HE10K, Mw 3.6×10^5 g mol^{-1}, Belgium) was dried at 110 °C overnight before use. *p*-Methylbenzenesulfonyl chloride (*syn*: tosyl chloride) and imidazole were obtained from Sigma-Aldrich while analytical grade solvents dimethylsulfoxide (DMSO), *N,N′*-dimethylacetamide (DMAc) and 1-propanol were purchased from Fluka and used without further purification. Disposable syringes (Injekt®, B. Braun) were used for collection of blood samples and dialysis membrane (regenerated cellulose; 21.0 mm dia; MWCO 12,000–14,000 Da) was obtained from Cellu•Sep® T4, USA.

2.2. Measurements

FT-IR spectra were recorded on Shimadzu IR Prestige-21 spectrometer using KBr pellet technique and pellets were dried under vacuum before analysis. ^{1}H NMR (64 scans) spectra were recorded on Bruker AVANCE 400 MHz and ^{13}C NMR (8000 scans) 75 MHz NMR spectrometers (Rheinstetten, Germany), using DMSO d_6 as the solvent.

The amount of FLB in conjugates **1**–**3** (drug contents; DC) was calculated by a Pharmaspec UV-1700 (Shimadzu, Japan) instrument at λ_{max} of 247 nm. Thermal analysis was performed on SDT Q 600 (TA Instruments, USA) at heating rate of 10 °C/min under N_2 from RT up to 800 °C. Transmission electron microscopy (TEM) was performed on TEM Philips 420 to study nano-assembly of HEC-FLB conjugates at an acceleration voltage of 120 kV. Bioequivalence studies were carried out on an HPLC/UV (Agilent, 1200 Series, Germany) instrument having degasser (G1322A), pump (G1311A), Shim-Pack column (ODS 5 μm; 4.6 × 250 mm) and UV–Vis detector (G1315B DAD).

2.3. Synthesis of HEC-FLB conjugate 2: A typical example

DMAc (30 mL) was heated in a round bottom flask at 80 °C and HEC (1.0 g, 3.62 mmol) was added with stirring and heating (80 °C, 30 min) to obtain an optically clear solution. Imidazole (0.99 g, 14.48 mmol), tosyl chloride (1.38 g, 7.24 mmol) and FLB (1.77 g, 7.24 mmol) were then added to the HEC solution by parts and resultant mixture was stirred at 80 °C for 8 h to synthesize HEC-FLB conjugate **2**. Precipitates of products were isolated by adding the reaction mixture to 1-propanol (200 mL). The products were thoroughly washed with 1-propanol (100 mL) to remove side products and unreacted drug contents and dried under vacuum at 50 °C before further analysis. Similar reaction procedure was adopted for the syntheses of HEC-FLB conjugates **1** and **3**.

DS (FLB) = 0.95 by UV–vis spectrophotometry; Yield: 1.39 g (78%); FTIR (KBr): 3213–3453 (OH), 2882 (CH), 1734 (CO_{ester}), 1429 (CH_2), 1047 (COC) cm^{-1}; ^{1}H NMR (400 MHz, DMSO d_6) δ ppm: 7.11–7.58 (H 11–22), 2.94–4.98 (H 1–8), 1.42 (H 23); ^{13}C NMR (75 MHz, DMSO d_6, NS 8000) δ ppm: 173.79 and 170.09 (C 9), 160.57 and 158.12 (C 13), 142.81 (C 11), 135.26 (C 17), 124.46–131.22 (C 15, 16, 18–22), 120.15 (C 14), 116.72 (C 12), 102.37–103.04 (C 1), 80.05–83.26 (C 2–4), 71.91–75.81 (C 5), 68.66 (C 6, 7), 60.68 (C 8), 44.35 (C 10), 18.86–21.28 (C 23).

Analytical data for sample **1**

DS = 0.40 by UV/Vis spectrophotometry; Yield: 0.97 g (73%); FTIR (KBr): 3276–3495 (OH), 1729 (CO_{Ester}), 1447 (CH_2), 1054 (COC) cm^{-1}.

Analytical data for sample **3**

DS = 1.74 by UV/Vis spectrophotometry; Yield: 1.85 g (76%); FTIR (KBr): 3286–3485 (OH), 1731 (CO_{Ester}), 1441 (CH_2), 1050 (COC) cm^{-1}.

Chemical shift values of HEC-FLB conjugates **1** and **3** were found comparable to conjugate **2** in ^{1}H and ^{13}C NMR spectra.

2.4. Determination of DC and DS

UV/Vis spectrophotometric analysis was used for the evaluation of DC of conjugates **1**–**3**. In a typical experiment, a calibration curve was plotted using standard solutions of FLB

in 0.1 N aq. NaOH. Sample was prepared by separately dissolving HEC-FLB conjugates **1**–**3** (10 mg each) in 0.1 N aq. NaOH (10 mL) and heating at 80 °C for 10 h. Volume of sample was made up to 10 mL using 0.1 N aq. NaOH after hydrolysis and absorbance was recorded at 247 nm (λ_{max}) after suitable dilution (to stay within the range of calibration curve). DC was determined by comparing the absorbance of sample with calibration curve of the standard. DS of FLB onto HEC was also calculated by acid base titration after saponification using reported method (Abbas et al., 2016) and found in good agreement with the values of DS drawn from DC.

2.5. Transmission electron microscopic (TEM) analysis

Nanoassemblies of HEC-FLB conjugate **2** were prepared using dialysis process. For this purpose, conjugate **2** (10 mg) was dissolved in DMSO (10 mL) and dialyzed against milli-Q water for 3 days. Dialyzing medium was periodically replaced with fresh milli-Q water during the course of experiment. After 3 days, the resultant slurry was diluted with milli-Q water, drop casted on a TEM grid (copper wired) and dried to record the TEM images.

2.6. Thermal analysis and degradation kinetics

TG curves of FLB and HEC-FLB conjugate **2** were used to calculate initial (Tdi), maximum (Tdm) and final (Tdf) thermal decomposition temperatures. The thermal data was used to calculate thermal degradation kinetics of drug FLB and conjugate **2** using Chang (Eq. (1); Chang 1994), Broido (Eq. (2); Broido 1969), Friedman (Eq. (3); Friedman, 1964) and Kissinger (Eq. (4); Kissinger, 1957) models.

$$\ln\left[\frac{\frac{d\alpha}{dt}}{(1-\alpha)^n}\right] = \ln Z - \frac{E_a}{RT} \tag{1}$$

$$\ln\left[\ln\left(\frac{1}{y}\right)\right] = \left(\frac{E_a}{RT}\right) + \text{constant} \tag{2}$$

$$\ln\left(\frac{d\alpha}{dt}\right) = \ln Z + n\ln(1-\alpha) - \frac{E}{RT} \tag{3}$$

$$S = \left[\frac{\left(\frac{d^2\alpha}{dt^2}\right)_L}{\left(\frac{d^2\alpha}{dt^2}\right)_R}\right] \tag{4}$$

where, in above equations, $d\alpha/dt$ represents rate of weight loss, W_o, W_∞ and W_t are initial, final and weight at particular temperature, respectively, $1-\alpha$ is residual weight of sample at a given temperature, T is absolute temperature, n is reaction order, R is ideal gas constant, E_a is energy of activation, Z is frequency factor, S is shape index while subscripts L and R represent values at left and right inflection points, respectively.

Shape index was used to calculate order of reaction by Eqs. (5) and (6).

$$n = 1.88S (S \geqslant 0.45) \tag{5}$$

$$n = 1.26S^{0.5} (S \leqslant 0.45) \tag{6}$$

Kinetic parameters like Z, n and E_a were calculated for thermal degradation of FLB and HEC-FLB conjugate **2** as explained by Hussain et al. (2017) for other conjugates of NSAIDs. Entropy change (ΔS), enthalpy change (ΔH) and free energy change (ΔG) were calculated using Eyring-Polanyi equation (Eyring and Polanyi, 1931). Doyle's method (Doyle, 1961) was used to calculate index of intrinsic thermal stability (ITS) and integral procedural decomposition temperature (IPDT) values.

2.7. High performance liquid chromatography (HPLC/UV) method development

A reverse phase HPLC/UV method was developed and validated for estimation of plasma concentration of FLB in rabbit models following oral administration of the FLB and conjugate **2**. Values of the HPLC/UV parameters for determination of FLB are shown in Supplementary Information (Table S1).

2.8. Pharmacokinetic studies

2.8.1. Participants and study design

Bioavailability of FLB from HEC-FLB conjugate **2** was studied by HPLC/UV method using rabbit models. For this purpose, twelve male albino rabbits (≈2 kg each) were divided into two groups, i.e., test and control. Animals in both groups were alternately kept under 12 h light and dark cycles and fasted for 10 h before experiment. In a typical experiment, the control group was orally given FLB (10 mg/kg body weight) and test group was orally administered with HEC-FLB conjugate **2** (45 mg; equivalent to 10 mg drug/kg body weight) as aqueous suspension (10 mL) using gavage tube. The animals were given free access to water and standard green food after 1 and 5 h of dosage, respectively.

National Institute of Health's Guidelines for the Care and Use of Laboratory Animals were followed for animal studies. Protocols of animal studies were approved form Pharmacy Research Ethics Committee, University of Sargodha, Sargodha, Pakistan.

2.8.2. Specimen collection and storage

Blood samples (3–5 mL) were collected from jugular veins of control and test animals with heparinized disposable syringes after 0.25, 0.5, 1.0, 2.0, 4.0, 6.0, 8.0, 12.0 and 18.0 h of dose administration. The samples were centrifuged at 3000*g* for 5 min and supernatant plasma was collected with micropipette. The extracted plasma was placed in a test tube, wrapped in aluminium foil and refrigerated till HPLC/UV assay.

2.8.3. Pharmacokinetic parameters

For HPLC/UV analysis, proteins were precipitated from the plasma samples by adding acetonitrile and methanol (1.0 mL each). The samples were centrifuged at 3000*g* for 5 min and clear supernatant was collected using micropipette. Collected samples were filtered through nylon syringe filter (0.45 μ) and used for HPLC/UV analysis.

Plasma concentration of FLB was plotted against time and area under the curve (AUC) was calculated using linear trapezoidal method (Shargel et al. 2012). Kinetic parameters like half-life of drug ($t_{1/2}$), clearance (Cl), volume of distribution (Vd) and peak drug concentration (C_{max}) were determined from AUC.

2.9. Bioassays

2.9.1. Carrageenan-induced paw edema

Paw edema test was used to determine anti-inflammatory potential of the synthesized HEC-FLB conjugate **2**. For this experiment, 12 BALB/c mice (20–25 g each) were divided into test and control group and acclimatized (25 °C; 50–60% humidity) for 10 days in stainless steel cages. Animals were given free access to standard rodent food and water during this period and kept under 12 h light and dark cycles before experiment. For paw edema test, the test group was given HEC-FLB conjugate **2** (equivalent to 10 mg/kg body weight, 1 mL/rat) and control group was given distilled water (0.5 mL/rat). Edema was induced by injecting the right hind paw of animals with saline suspension of carrageenan (1%, 0.1 mL) after 1 h of dose administration and volume of paw was measured after 1, 2, 3, 4 and 6 h of injection using plethysmometer (Basile, Comerio, Italy). Difference between volume of normal and swollen paws was used to calculate percentage inhibition of edema and percentage swelling.

2.9.2. In vitro cytotoxicity assay

Cytotoxic profile of HEC-FLB conjugate **2** was determined using 3-(4,5-dimethylthiazole-2-*yl*)-2,5-diphenyltetrazolium bromide (MTT) assay (Berridge and Tan, 1993). For this purpose, culture plates were prepared using fetal bovine serum (10% v/v), 1% penicillin and streptomycin, α-MEM and Fungizone (2.5 μg mL^{-1}) and L929 cell lines were incubated to these plates at 37 °C. Culture wells were divided into three groups, conjugate solutions (2, 4, 6, 8 or 10 mM) were added and allowed to stand for 24, 48 and 72 h. After the specified time, supernatant from each culture plate was replaced with MTT solution (10 μL, 0.5 mg mL^{-1}), plates were incubated at 37 °C for 4 h and the MTT solution was replaced with DMSO (100 μL). Absorbance was then recorded using a PowerWave™ Microplate spectrophotometer (BioTek, USA) at 570 nm and percentage of cell viability was calculated using Eq. (7).

$$\%viability = \frac{A_T}{A_C} \times 100 \tag{7}$$

where A_C is optical density of control and A_T is optical density of treated cells.

2.9.3. Cytokine release assay

Immunomodulatory properties of HEC-FLB conjugate **2** were determined using cytokine release assay. For this purpose, macrophages (THP-1 cell lines) were cultured in a medium containing phenyl mercuric acetate (PMA, 10 ng/mL) for 24 h and incubated in RPMI-1640 having 100 mg of streptomycin per mL with 25 mM 4-(2-hydroxyethyl)-1-piperazineethanesulfonic acid (HEPES), 10% fetal bovine serum, 100 mg of penicillin per mL and 2 mM L-glutamine. Cells were then placed in 100 nM PMA for 24 h to allow differentiation, washed with RPMI and incubated in 10% fetal bovine serum with and without lipopolysaccharides (LPS). After differentiation, cells were incubated in wells containing test compounds or vehicle (0.5% DMSO) for 30 min at 37 °C. Finally, 20 μL of LPS (10 μg mL^{-1}) was added to a final concentration of 1 μg/mL and cytokine release was measured.

2.10. Statistical analyses

Statistical analysis was performed using GraphPad Prism 5.0 (GraphPad Software Inc., La Jolla, CA, USA) while two-way ANOVA trailed by multiple-comparison test was used for data analysis. A "p" value < 0.05 was considered statistically significant and denoted by asterisks in the respective figures.

3. Results and discussion

3.1. Synthesis and characterization HEC-FLB conjugates

Amphiphilic conjugates of FLB on to HEC were fabricated using tosyl chloride as *in situ* activating agent. The carboxyl group on FLB was converted into tosylate intermediate which was further reacted with pre-dissolved HEC in presence of imidazole base to yield esterified prodrugs, i.e., HEC-FLB conjugates **1**–**3**. Present reaction methodology appeared efficient as conjugates showed moderate to high DS of FLB (0.40–1.74 by UV/Vis and 0.38–1.70 by acid base titration) on to HEC with high reaction yields (73–78%). A generalized reaction methodology for the synthesis of HEC-FLB conjugates **1**–**3** is illustrated in Fig. 1 while conditions and results of reactions are summarized in Table 1.

Structure of synthesized HEC-FLB conjugates was characterized using FT-IR spectroscopy. HEC-FLB conjugate **2** showed ester signals at 1734 cm^{-1} while CH_2 absorptions were detected at 1429 cm^{-1}. The unmodified hydroxyls on HEC backbone were observed in the range of 3387–3453 cm^{-1} and COC was observed at 1047 cm^{-1}. FT-IR spectra of conjugates **1** and **3** showed prominent absorptions at 1732 and 1737 cm^{-1} indicating presence of ester functions in the said conjugates. Overlay FT-IR spectra of FLB and HEC-FLB conjugate **2** are depicted in Fig. 2.

Structure of HEC-FLB conjugates **1**–**3** was further characterized by recording their ^{1}H NMR (400 MHz, DMSO d_6) spectra. Spectrum of sample **2** showed presence of aromatic protons in the conjugate as chemical shifts were detected in the range of δ 7.11–7.58 (H 12, 15, 16, 18–22) ppm. Methyl group of FLB was detectable at δ 1.42 (H 23) and HEC backbone signals were observed in the range of 2.94–4.98 (H 1–8) ppm. These results indicated that aromatic system of FLB showed broad signals which indicated the covalent attachment of FLB on to HEC. Comparable chemicals shift values were observed in the ^{1}H NMR spectra of conjugate **1** and **3** as well. ^{1}H NMR spectrum of HEC-FLB conjugate **2** is depicted in Fig. 3 as a typical example.

Formation of HEC-FLB conjugate **2** was established form ^{13}C NMR (75 MHz, DMSO d_6) spectrum where characteristic signals of ester carbonyl was detected at δ 173.79–170.09 (C 9) ppm. Fluorinated carbon of FLB was observed at δ 160.57 and 158.12 (C 13) ppm and other aromatic carbons were detected at δ 142.81 (C 11), 135.26 (C 17), 124.46–131.22 (C 15, 16, 18–22), 120.15 (C 14) and 116.72 (C 12) ppm. The CH adjacent to acyl group of FLB appeared at δ 44.35 (C 10) ppm, while methyl group was observed at δ 18.86–21.28 (C 23) ppm. HEC repeating units were detected at δ 102.37–103.04 (C 1), 80.05–83.26 (C 2–4), 71.91–75.81 (C 5), 68.66 (C 6, 7) and 60.68 (C 8) ppm. Spectra of HEC-FLB conjugates **1** and **3**

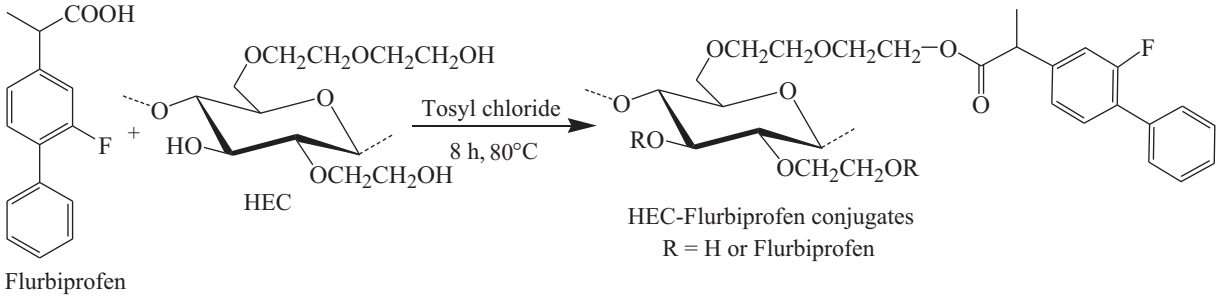

Fig. 1 Synthesis of HEC-FLB conjugates using tosyl chloride.

Table 1 Reaction conditions and results for the synthesis of HEC-FLB conjugates.

Samples	Molar Ratio[a]	DC[b]	DS[c]	DS[d]	Yield (%/g)	Solubility
1	1:1:1:2	25	0.40	0.38	73/0.97	DMF, DMSO, DMAc
2	1:2:2:4	44	0.95	0.92	78/1.39	DMF, DMSO, DMAc
3	1:4:4:8	59	1.74	1.70	76/1.85	DMF, DMSO, DMAc

[a] HEC repeating unit (HRU): FLB: tosyl chloride: imidazole.
[b] DC (mg drug/100 mg of conjugate) calculated by UV/Vis spectroscopy.
[c] DS calculated from DC in terms of substitution of drug per HRU.
[d] DS calculated by acid base titration after saponification.

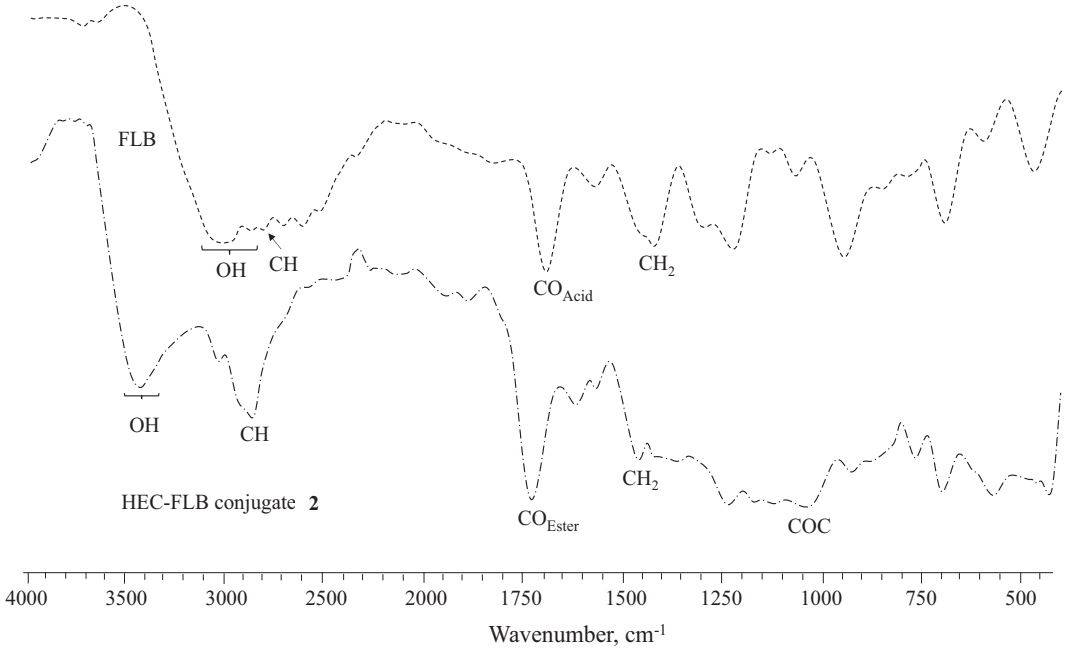

Fig. 2 Overlay FTIR (KBr) spectra of FLB and HEC-FLB conjugate **2**.

showed comparable chemical shift values to conjugate **2**. A typical ^{13}C NMR spectrum of sample **2** is shown in Fig. 4.

3.2. Transmission electron microscopic (TEM) analysis

Esterification of hydrophobic drugs like NSAIDs on to hydrophilic polymers like cellulose ethers imparts amphiphilic properties to the resultant conjugates. Such conjugates are known to show various morphologies at solvent interface due to altered/adjusted hydrophilic properties (Hussain et al., 2017). So, TEM images of HEC-FLB conjugates **1**–**3** were recorded to determine their morphology after dialysis at water/DMSO interface. Only conjugate **2** showed formation of nanoparticles in the size regimen of 220–550 nm (Fig. 5) in the TEM images while conjugates **1** and **3** did not show well-defined morphology. Such nanoassembled drugs may be exploited as potential devices for achieving increased drug internalization at the target site.

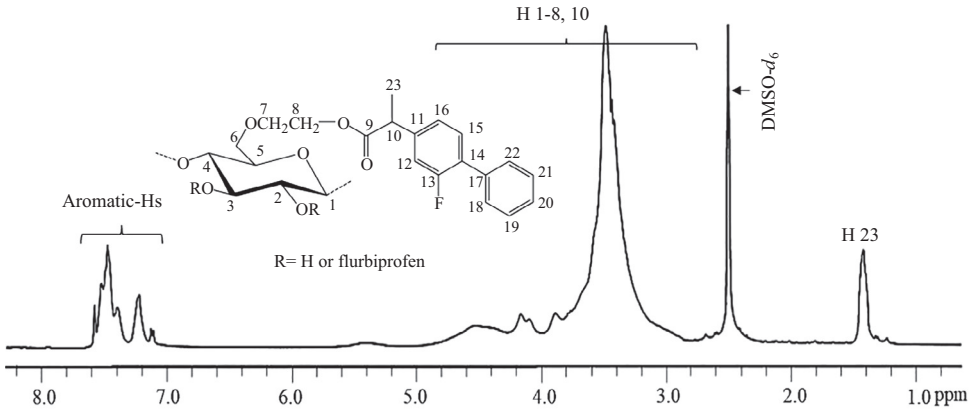

Fig. 3 ^{1}H NMR (400 MHz, DMSO d_6) spectrum of HEC-FLB conjugate **2**.

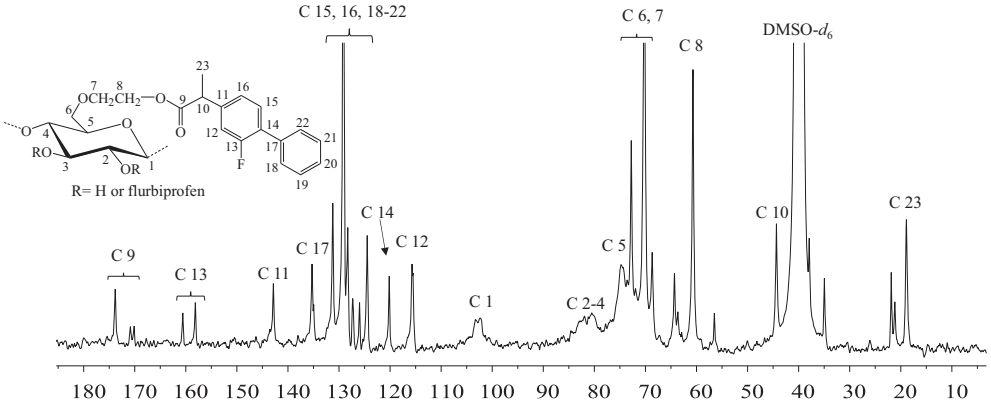

Fig. 4 ^{13}C NMR (400 MHz, DMSO d_6) spectrum of HEC-FLB conjugate **2**.

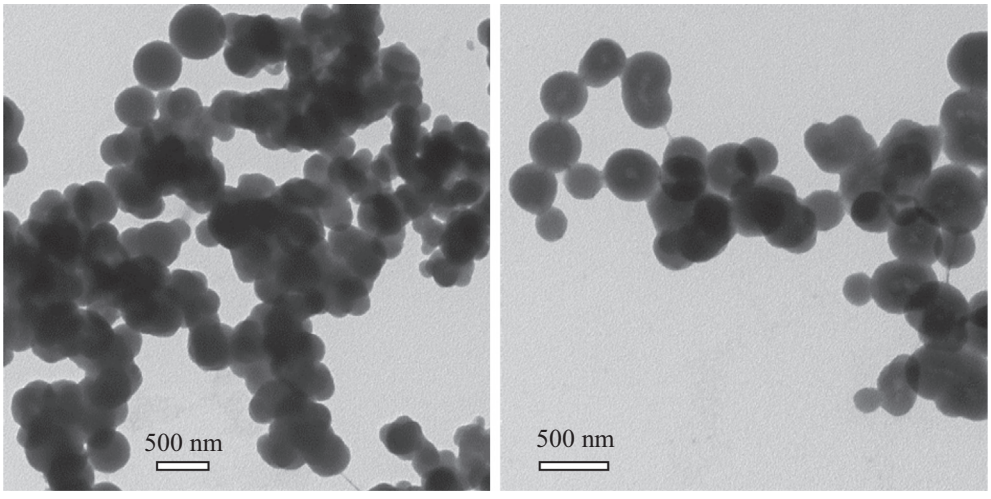

Fig. 5 TEM images of HEC-FLB conjugate **2**.

3.3. Pharmacokinetic studies

Plasma levels of FLB in rabbit model were determined using validated reverse phase HPLC/UV method. Results of method validation parameters are given in Supplementary Information (see Table S1).

A single oral dose of conjugate **2** (45 mg, equivalent to 10 mg drug/kg body weight) was given to rabbits per oral route and plasma concentration vs. time curve was plotted. The plot showed $AUC_{0-\infty}$ value of 113.43 h μg mL^{-1} while t_{max} and $t_{1/2}$ were found to be 4.0 and 10.63 h, respectively. These values of t_{max} and $t_{1/2}$ of FLB from the conjugate are considerably

higher than unmodified drug (2.0 and 4.89 h, respectively). Vd and Cl of FLB from the conjugate were found to be 2.70 L kg^{-1} and 0.18 L h^{-1}, respectively. The values of pharmacokinetic parameters revealed that conjugate **2** shows enhanced bioavailability of FLB and could be used to achieve sustained release of drug. The conjugate could also maintain therapeutic levels of drug for longer period of time than unmodified drug as indicated from increased $t_{1/2}$ value of conjugate. These results are, of course, important for reducing dosage frequency and associated side-effects in case of prolonged FLB therapy. The overlay plasma concentration vs. time curve showing bioavailability of FLB from control and conjugate **2** is shown in Fig. 6 and values of pharmacokinetic parameters are listed in Table 2.

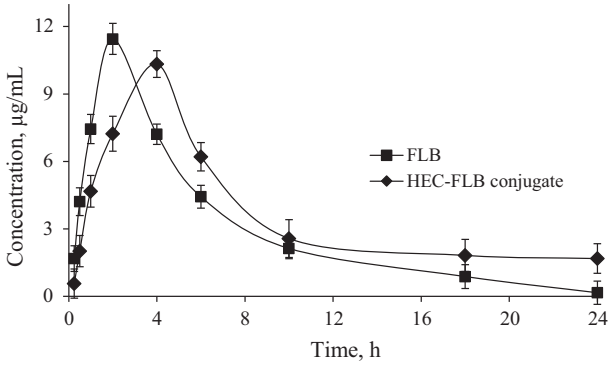

Fig. 6 Plasma concentrations vs. time curve of standard FLB and FLB from HEC-FLB conjugate **2** after single oral dose of 45 mg.

Table 2 Pharmacokinetic data of HEC-FLB conjugate **2** after a single oral dose of 45 mg.

Parameter	FLB	FLB from HEC-FLB conjugate **2**
t_{max} (h)	2.0	4.0
C_{max} (µg mL^{-1})	11.45 ± 1.87	10.33 ± 1.63
$t_{1/2}$ (h)	4.89 ± 1.03	10.63 ± 0.97
$AUC_{0-\infty}$ (h µg mL^{-1})	73.88 ± 3.67	113.43 ± 6.73
V_d (L kg^{-1})	1.91 ± 0.27	2.70 ± 0.53
Cl (L h^{-1})	0.27 ± 0.03	0.18 ± 0.06

3.4. Carrageenan-induced paw edema

Anti-inflammatory potential of newly synthesized HEC-FLB conjugate **2** was assessed from inhibition of edema in BALB/c mice. Significant reduction in swelling% of paw volume was observed in test animals (79% inhibition) as compared

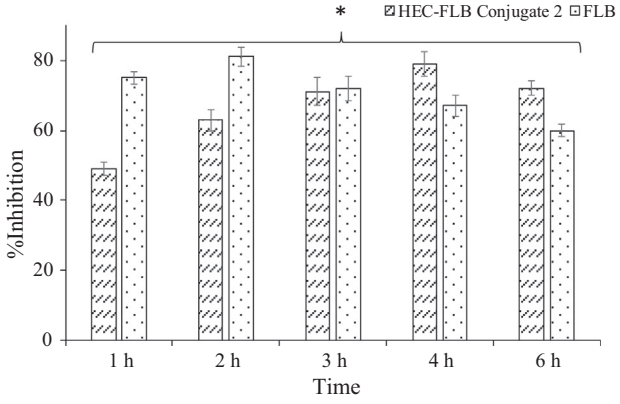

Fig. 7 Carrageenan induced paw edema inhibition vs. time for HEC-FLB conjugate **2** (% inhibition vs. water-only control). Statistically significant when compared to control indicated with * $p < 0.05$.

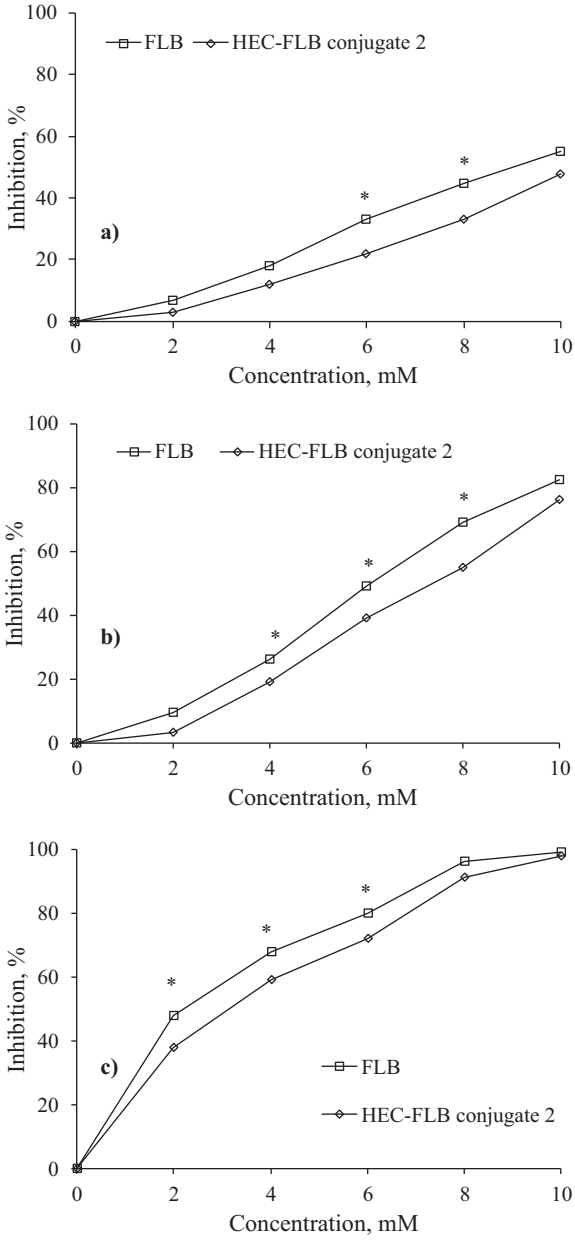

Fig. 8 Cytotoxic effects (inhibition, %) by different concentrations of FLB and conjugate **2** on L929 cell line after 24 (a), 48 (b) and 72 h (c). * $p < 0.05$ is considered significant when compared to control.

to controls (water only) up to 4 h following carrageenan injection. The results indicated that anti-inflammatory properties of FLB were retained after attachment on to HEC with additional advantage of sustained release. Results of% inhibition of edema caused by conjugate **2** and FLB at various time points are shown in Fig. 7.

3.5. In vitro cytotoxicity assay

Cytotoxic potential of HEC-FLB conjugate **2** was studied using MTT assay. No significant cytotoxicity was observed against L929 cell lines up to 24 h when exposed to conjugate **2** in the concentration range of 2–10 mM. However, significant reduction of mitochondrial enzymes was observed when cell lines were exposed to conjugate for 48 and 72 h. Since this period is well above the clearance time of FLB, so it was inferred that conjugate **2** is non-cytotoxic hence biocompatible within the time it is likely to remain in human body. Cytotoxic effect of various concentrations of standard FLB and conjugate **2** at various exposure times has been illustrated in Fig. 8.

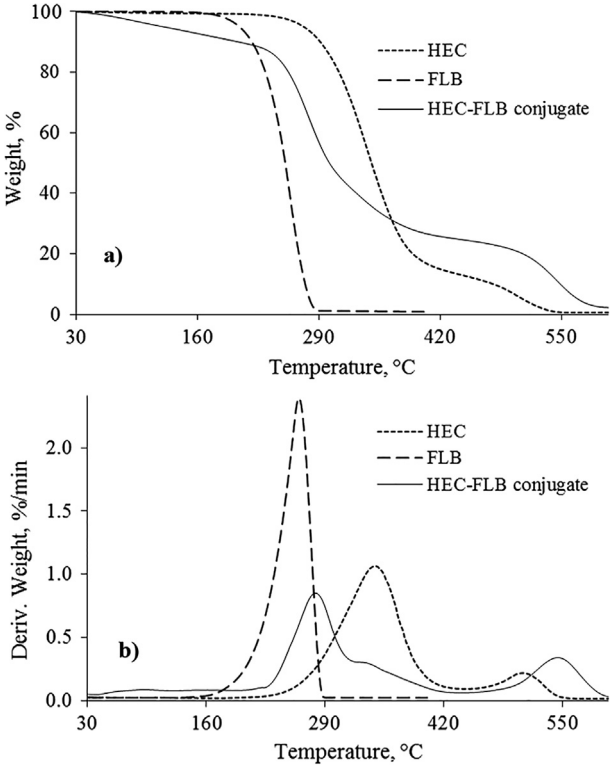

Fig. 9 Overlay TG (a) and DTG (b) curves FLB and HEC-FLB conjugate **2.**

3.6. Cytokine release assay

NSAIDs are known to modulate cytokine release from stimulated macrophages and act as effective COX inhibitors. Inhibitory effect of HEC-FLB conjugate **2** on release of tumor necrosis factor-α (TNF-α) and interleukin-6 (IL-6) from THP-1 cell lines was studied to evaluate their immunomodulatory properties. Supernatant from THP-1 cultures showed 34 and 36% inhibition in the levels of IL-6 and TNF-α, respectively which is comparable with FLB (30 and 32%, respectively). These results indicated that HEC-FLB conjugate **2** could be exploited as a potent immunomodulatory agent.

3.7. Thermal analyses and degradation kinetics

Thermal analysis is becoming increasingly popular to determine performance parameters of drug during formulation design, storage and handling, etc (Giron, 2002). Since polymers are macromolecular matrices, so it is expected that conjugation on to macromolecular backbone would impart thermal stability to drug (Hussain et al., 2017). Therefore, synthesized HEC-FLB conjugate **2** was subjected to thermal analysis to assess its thermal stability and thermodynamic parameters. Single step thermal degradation of FLB started at 184 °C (Tdi) and completed at 283 °C (Tdf) with maxim weight loss at 260 °C (Tdm). In contrast, conjugate **2** showed two step degradation profile. First and major degradation step of conjugate **2** showed onset of weight loss at 227 °C (Tdi) that ended at 392 °C (Tdf) with maximum degradation at 244 °C (Tdm) and weight loss of 60.35%. Minor degradation of conjugate **2** occurred in second step with Tdm value of 543 °C accompanying a weight loss of 26.96%. Thermal decomposition of FLB ended at 400 °C leaving 0.86% char yield while decomposition of conjugate **2** ended at 700 °C with 1.97% char yield. Increased Tdi values (43 °C) of first degradation step of conjugate **2** and appearance of new step at significantly higher temperature range (496–577 °C) indicated that thermal stability of FLB was increased after conjugate formation. Fig. 9 shows overlay TG and DTG curves of FLB and conjugate **2** while Tdi, Tdm and Tdf values are given in Table 3.

Thermal kinetics were applied to evaluate kinetic parametres of degradation of FLB and HEC-FLB conjugate **2**. Friedman, Broido and Chang models showed *Ea* values of 98.82, 104.75 and 98.70 kJ mol^{-1}, respectively for degradation of FLB while first and major degradation step of conjugate **2** showed *Ea* values of 112.59, 112.24 and 111.90 kJ mol^{-1},

Table 3 Thermal analysis, degradation kinetics and thermodynamic parameters of HEC-FLB conjugate **2**.

Sample	Thermal degradation temperatures		Thermal degradation kinetics						Thermodynamic parameters		
	Tdi, Tdm, Tdf	Weight loss (%) at Tdf	Method	Step	R^2	n	E_a (kJ mol^{-1})	ln$Z$	ΔH (kJ mol^{-1})	ΔS (J K^{-1})	ΔG (kJ mol^{-1})
HEC-FLB conjugate **2**	227, 244, 392	60.35	Friedman	I	0.999	–	112.59	25.50	108.28	−49.37	133.82
			Broido	I	0.999	–	112.24	25.54	107.94	−49.07	133.31
			Chang	I	0.999	1	111.90	26.85	107.60	−38.20	127.36
			Kissinger	I	–	1.52	–	–	–	–	–

respectively for the said models. Thermal degradation of FLB and conjugate **2** was found to follow 1st order kinetics as per Chang and Kissinger models (see Table 3).

Thermodynamic parameters like ΔH, ΔS and ΔG were calculated for degradation of drug and conjugate using Eyring-Polanyi equation (see Table 3). Doyle's method showed that FLB and conjugate **2** showed IPDT values of 271 and 355, respectively while ITS values were found to be 0.37 and 0.43, respectively. Comparison of thermograms of drug and conjugate and values of thermodynamic parameters indicated that attachment of FLB on to polymeric backbone imparted significant thermal stability to the drug. Such thermally stable prodrugs could be potential for achieving enhanced performance parameters of drugs like increased shelf-life, etc.

4. Conclusions

FLB conjugates based on HEC were successfully synthesized and thoroughly characterized. Pharmacokinetic studies revealed that bioavailability of FLB was enhanced after attachment on to polymer backbone and the conjugate showed sustained release characteristics. HEC-FLB conjugates were noticed to be potent anti-inflammatory agents with pronounced immunomodulatory properties. Conjugates showed no cytotoxicity over the clearance time of FLB from human body in MTT assay. Enhanced thermal stability imparted to FLB after conjugate formation could be effective for achieving improved performance parameters of drug during formulation design, storage and handling. Such prodrug systems may be further exploited as efficient devices to achieve sustained release of FLB and other NSAIDs. By forming such prodrugs of different NSAIDs, modeling this study, one may alleviate NSAID associated gastric irritancy and get improved pharmacokinetic profile.

Acknowledgement

K. Abbas gratefully acknowledges financial support provided by the Higher Education Commission (HEC) of Pakistan under "HEC Indigenous 5000 fellowships Scheme". FLB was generously gifted by Candid Pharmaceuticals Sialkot, Pakistan.

Appendix A. Supplementary material

Supplementary data associated with this article can be found, in the online version, at https://doi.org/10.1016/j.arabjc.2018.03.011.

References

Abbas, K., Amin, M., Hussain, M.A., Sher, M., Bukhari, S.N.A., Jantan, I., Edgar, K.J., 2017a. Designing novel bioconjugates of hydroxyethylcellulose and salicylates for potential pharmaceutical and pharmacological applications. Int. J. Biol. Macromol. 103, 441–450.

Abbas, K., Amin, M., Hussain, M.A., Sher, M., Bukhari, S.N.A., Edgar, K.J., 2017b. Design, characterization and pharmaceutical/pharmacological applications of ibuprofen conjugates based on hydroxyethylcellulose. RSC Adv. 7 (80), 50672–50679.

Abbas, N.S., Amin, M., Hussain, M.A., Edgar, K.J., Tahir, M.N., Tremel, W., 2016. Extended release and enhanced bioavailability of moxifloxacin conjugated with hydrophilic cellulose ethers. Carbohydr. Polym. 136, 1297–1306.

Amin, M., Abbas, N.S., Hussain, M.A., Edgar, K.J., Tahir, M.N., Tremel, W., Sher, M., 2015. Cellulose ether derivatives: a new platform for prodrug formation of fluoroquinolone antibiotics. Cellulose 22, 2011–2022.

Berridge, M.V., Tan, A.V., 1993. Characterization of the cellular reduction of 3- (4,5-dimethylthiazol-yl)-2,5-diphenyitetrazolium bromide (MTT): Subcellular localization, substrate dependence and involvement of mitochondrial electron transport in MTT reduction. Arch. Biochem. Biophys. 303, 474–482.

Broido, A., 1969. A simple, sensitive graphical method of treating thermogravimetric analysis data. J. Polym. Sci. Part A-2: Polym. Phys. 7, 1761–1773.

Chang, W.L., 1994. Decomposition behavior of polyurethanes via mathematical simulation. J. Appl. Polym. Sci. 53, 1759–1769.

Doyle, C.D., 1961. Estimating thermal stability of experimental polymers by empirical thermogravimetric analysis. Anal. Chem. 33, 77–79.

Eyring, H., Polanyi, M., 1931. Über Einfache Gasreaktionen. Z. Phys. Chem. B. 12, 279–311.

Friedman, H.L., 1964. Kinetics of thermal degradation of char-forming plastics from thermogravimetry: Application to a phenolic plastic. J. Polym. Sci. Part C: Polym. Symp. 6, 183–195.

Gabriel, S.E., Jaakkimainen, L., Bombardier, C., 1991. Risk for serious gastrointestinal complications related to use of nonsteroidal anti-inflammatory drugs. A meta-analysis. Ann. Int. Med. 115 (10), 787–796.

Giron, D., 2002. Applications of thermal analysis and coupled techniques in pharmaceutical industry. J. Therm. Anal. Calorim. 68, 335–357.

Halen, P.K., Chagti, K.K., Giridhar, R., Yadav, M.R., 2006. Synthesis and pharmacological evaluation of some dual-acting amino-alcohol ester derivatives of flurbiprofen and 2-[1,1'-biphenyl-4-yl]acetic acid: a potential approach to reduce local gastrointestinal toxicity. Chem. Biodivers. 3 (11), 1238–1248.

Halen, P.K., Murumkar, P.R., Giridhar, R., Yadav, M.R., 2009. Prodrug designing of NSAIDs. Mini – Rev. Med. Chem. 9 (1), 124–139.

Harboe, E., Larsen, C., Johansen, M., 1988. Macromolecular prodrugs X. bioavailability of naproxen after oral administration of dextran-naproxen ester conjugates in rabbits. Farmaci. Sci. Ed. 16, 65–72.

Hussain, M.A., Abbas, K., Lodhi, B.A., Sher, M., Ali, M., Tahir, M. N., Tremel, W., Iqbal, S., 2017. Fabrication, characterization, thermal stability and nanoassemblies of novel pullulan-aspirin conjugates. Arab. J. Chem. 10 (2), S1597–S1603.

Kissinger, H.E., 1957. Reaction kinetics in differential thermal analysis. Anal. Chem. 29, 1702–1706.

Larsen, C., 1990. Dextran prodrugs; physicochemical and chemical aspects in relation to in-vivo properties (DSc Thesis), Villadsen and Christensen, Copenhagen, Denmark, 1990, pp. 81–82.

Li, D., Ding, J., Zhuang, X., Chen, L., Chen, X., 2016. Drug binding rate regulates the properties of polysaccharide prodrugs. J. Mater. Chem. B 4, 5167–5177.

Li, D., Han, J., Ding, J., Chen, L., Chen, X., 2017. Acid-sensitive dextran prodrug: A higher molecular weight makes a better efficacy. Carbohydr. Polym. 161, 33–41.

Mørk, N., Bundgaard, H., 1992. Stereoselective enzymatic hydrolysis of various ester prodrugs of ibuprofen and flurbiprofen in human plasma. Pharmaceut. Res. 9 (4), 492–496.

Shargel, L., Pong, S.W., Yu, A.B.C., 2012. Introduction to biopharmaceutics and pharmacokinetics. Applied Biopharmaceutics and Pharmacokinetics. The McGraw-Hill Companies Inc., USA.

Xu, W., Ding, J., Xiao, C., Li, L., Zhuang, X., Chen, X., 2015. Versatile preparation of intracellular-acidity-sensitive oxime-linked polysaccharide-doxorubicin conjugate for malignancy therapeutic. Biomaterials 54, 27–86.